

Finite-size effects on the static properties of a single-chain magnet

L. Bogani,^{1,*} R. Sessoli,^{1,†} M. G. Pini,² A. Rettori,³ M. A. Novak,⁴ P. Rosa,^{1,‡} M. Massi,⁵ M. E. Fedi,⁵ L. Giuntini,⁵ A. Caneschi,¹ and D. Gatteschi¹

¹*Dipartimento di Chimica and INSTM, Università di Firenze, Via della Lastruccia 3, I-50019 Sesto Fiorentino, Italy*

²*Istituto dei Sistemi Complessi, Sezione di Firenze, Consiglio Nazionale delle Ricerche, Via Madonna del Piano, 50019 Sesto Fiorentino (FI), Italy*

³*Dipartimento di Fisica and u.d.r. INFN, Università di Firenze, Via G. Sansone 1, I-50019 Sesto Fiorentino, Italy*

⁴*Instituto de Fisica, Universidade Federal do Rio de Janeiro, CP68528, RJ 21945-970, Brazil*

⁵*Dipartimento di Fisica and u.d.r. INFN, Università di Firenze, I-50019 Sesto Fiorentino, Italy*

(Received 5 March 2005; revised manuscript received 20 May 2005; published 3 August 2005)

We study the role of defects in the “single-chain magnet” CoPhOMe by inserting a controlled number of diamagnetic impurities. The samples are analyzed with unprecedented accuracy with the particle induced x-ray emission technique, and with ac and dc magnetic measurements. In an external applied field the system shows an unexpected behavior, giving rise to a double peak in the susceptibility. The static thermodynamic properties of the randomly diluted Ising chain with alternating g values are then exactly obtained via a transfer matrix approach. These results are compared to the experimental behavior of CoPhOMe, showing qualitative agreement.

DOI: [10.1103/PhysRevB.72.064406](https://doi.org/10.1103/PhysRevB.72.064406)

PACS number(s): 75.50.-y, 75.70.Rf, 75.30.Kz, 31.70.Ks

I. INTRODUCTION

The theoretical treatment of one dimensional (1D) models is significantly easier than that of two or three dimensional ones and, in many cases, it is the only one which leads to exact analytical solutions. A number of theoretical predictions concerning magnetic 1D materials could thus be made in the last three decades and many of them, even the most surprising ones, have been tested and successfully verified experimentally. To mention only a couple of examples Haldane’s conjecture¹ has been confirmed² in a variety of real compounds and solitons have been shown to play an important role in the properties of several easy plane quasi-1D systems.³ All these effects could be found in chemically simple systems, but, to move on in the study of low dimensional magnets, it has been necessary to shift to more sophisticated materials,⁴ whose properties can be selectively adjusted. In this regard molecular materials have already shown their great potential, allowing, thanks to the means of classical synthetic chemistry, for chemical modifications aimed to the desired behavior. In particular the organometallic polymeric systems formed by alternating nitronyl-nitroxide radicals and transition metal or rare earth ions, although already extensively studied,⁵ still seem to hold unexplored potential. It is, for example, in an alternating gadolinium-nitronyl-nitroxide chain that the first experimental evidence of a chiral magnetic phase has recently been found.⁶

One of these systems, made of alternating Co(II) and radical paramagnetic centers, CoPhOMe, has recently attracted great attention as it is the archetypal massive magnetic material in which Glauber dynamics⁷ of the magnetization could be observed.^{8,9} This makes this system quite appealing as, at low temperature, slow relaxation of the magnetization and the opening of an hysteresis cycle without three dimensional (3D) magnetic order are observed. As this behavior is reminiscent of that observed in the more well-known class of

“single-molecule magnets” (SMMs),¹⁰ the name “single-chain magnets” (SCMs) has been proposed¹¹ for a class of compounds comprising CoPhOMe and similar recently developed materials.^{11–17}

In truth the possibility of observing Glauber dynamics is, at least at first glance, a paradox, as the two major assumptions of this dynamical model are a strong Ising-like anisotropy of the magnetic centers and the negligibility of interchain interactions J' in respect to the intrachain exchange coupling J . In Ising systems, however, the correlation length diverges exponentially on lowering the temperature and this, in a mean field treatment of interchain interactions,¹⁸ gives rise to the onset of 3D ordering at relatively high temperatures. It is easy to calculate that in an infinite Ising system with $|J|/k_B \approx 100$ K (as previously estimated for CoPhOMe) and a $|J'/J| = 10^{-4}$ ratio (which should be close to that of CoPhOMe), the transition temperature to 3D order is expected to be found close to 25 K, well above any observed dynamical regime. The fact that no phase transition is observable in SCMs down to very low temperatures could be due to the presence of naturally occurring defects, which impose a geometrical limit to the correlation length. It has already been observed, both experimentally and theoretically, that the presence of impurities or defects can dramatically reduce the onset of 3D ordering^{18,19} and significantly alter the static properties.²⁰

In an earlier letter²¹ we showed that naturally occurring or artificially introduced defects strongly influence the properties of CoPhOMe and pointed out that slow relaxation of the magnetization is observable even in small segments of chain. In this work we provide a more detailed investigation, both from the theoretical and experimental point of view, of finite-size effects on the static magnetic properties of CoPhOMe.

First of all we obtain, using a transfer matrix approach, the exact analytical expressions for the free energy of a randomly diluted ferrimagnetic Ising chain with spin $\sigma=1$ and alternating Landé g factors in zero field and in an external

applied field. We show that these results differ significantly from those obtained for isotropic and anisotropic quantum XY chains,^{22,23} displaying characteristic features. Incidentally it must be noticed that, although several models of 1D systems with exotic patterns of interaction or disorder have been studied, no work on finite-size effects in ferrimagnetic chains, that are the most common magnetic experimental systems, is available. We then present experimental data on CoPhOMe samples where a known amount of diamagnetic impurities has been inserted using chemical means and which have been accurately characterized with a particle induced x-ray emission (PIXE) analysis.²⁴ These results can be qualitatively explained with the theoretical analysis developed, especially if the observed trend of the dopant concentration is used in the calculation. We then analyze the behavior of Griffiths singularities^{25–27} on varying the difference between the Landé g factors and show that the doubling of the magnetic unit cell and the simultaneous breaking of translational invariance lead to a threefold splitting of the unique singularity found in ferromagnets and antiferromagnets.

II. EXACT THERMODYNAMICS OF THE RANDOMLY DILUTE FERRIMAGNETIC ISING CHAIN

A transfer matrix approach to ferromagnetic and antiferromagnetic Ising chains was developed by Matsubara and coworkers²⁸ and was later more deeply studied by Wortis,²⁵ who pointed out that the introduction of defects adds singularities of the Griffiths type²⁶ to the divergences of the thermodynamic quantities of the pure chains. The effect of dilution on the thermodynamics of classical Heisenberg and planar spin chains was then studied by Pini and Rettori²⁹ and Hu and McGurn³⁰ using an analogous classical transfer matrix method to explain experimental data from several dilute compounds.³¹ Here we will consider the ferrimagnetic Ising chain with alternating g values and only nearest-neighbor coupling interactions J . The spin Hamiltonian for the pure system is:

$$\mathcal{H} = - \sum_{i=1}^{N/2} [J(\sigma_{2i-1}\sigma_{2i} + \sigma_{2i}\sigma_{2i+1}) + \mu_B H(g_{Co}\sigma_{2i} + g_R\sigma_{2i-1})], \quad (1)$$

where g_{Co} and g_R are the two Landé factors (they correspond, respectively, to those of Co and radical spins of the experimental system), μ_B is the Bohr magneton, H is the external magnetic field, and $\sigma = \pm 1$, except for $\sigma_{N+1} = 0$. We shall concentrate only on random site dilution, in which each magnetic site of the chain is either substituted by a diamagnetic impurity (with probability C) or is left unchanged (with probability $1-C$), but the results we obtain can be trivially extended to bond dilution.²⁵ In our model we also assume that, as no next nearest neighbor interactions are present, the dilution splits the system into *noninteracting* segments of chain. Thus, after dilution, we can treat the whole system as a collection of independent finite chains of length L whose corresponding free energies $F_L(T, H)$, functions of the temperature T and of the external applied field H , are additive.

The free energy per site F can be computed by the expression^{25,26,28}

$$F = C^2 \sum_{L=1}^{\infty} (1-C)^L F_L(T, H). \quad (2)$$

To do this we must calculate the free energies $F_L(T, H)$ of the finite chains. It is convenient to define the basic matrices needed to describe the problem

$$\mathbf{S} = \begin{bmatrix} 1 & 1 \\ 0 & 0 \end{bmatrix}, \quad \mathbf{T}_J = \begin{bmatrix} e^{a_J} & e^{-a_J} \\ e^{-a_J} & e^{a_J} \end{bmatrix},$$

$$\mathbf{T}_R = \begin{bmatrix} e^{a_R} & 0 \\ 0 & e^{-a_R} \end{bmatrix}, \quad \mathbf{T}_{Co} = \begin{bmatrix} e^{a_{Co}} & 0 \\ 0 & e^{-a_{Co}} \end{bmatrix}, \quad (3)$$

where $a_{Co} = \beta \mu_B g_{Co} H$, $a_R = \beta \mu_B g_R H$, $a_J = \beta J$, and $\beta = (k_B T)^{-1}$. The products of matrices

$$\mathbf{P}_{Co} = \mathbf{T}_{Co}^{1/2} \mathbf{T}_J \mathbf{T}_R \mathbf{T}_J \mathbf{T}_{Co}^{1/2}$$

$$= \begin{bmatrix} 2e^{a_{Co}} \cosh(a_R + 2a_J) & 2 \cosh(a_R) \\ 2 \cosh(a_R) & 2e^{-a_{Co}} \cosh(a_R - 2a_J) \end{bmatrix},$$

$$\mathbf{P}_R = \mathbf{T}_R^{1/2} \mathbf{T}_J \mathbf{T}_{Co} \mathbf{T}_J \mathbf{T}_R^{1/2}$$

$$= \begin{bmatrix} 2e^{a_R} \cosh(a_{Co} + 2a_J) & 2 \cosh(a_{Co}) \\ 2 \cosh(a_{Co}) & 2e^{-a_R} \cosh(a_{Co} - 2a_J) \end{bmatrix} \quad (4)$$

are Hermitian symmetric matrices and have identical right and left eigenvectors. They can thus be used as convenient transfer matrices to evaluate the partition function, since the properties of completeness and orthonormality are applicable in a straightforward way. In writing the partition function Z_L of a chain of length L we must only take care to consider even and odd segments separately and notice that, for the latter, we must make a distinction between segments beginning (and ending) with a radical or with a cobalt site. The three partition functions take the form

$$Z_L = \begin{cases} Z_{Odd}^{Co} = \text{tr} |\mathbf{S} \mathbf{T}_{Co}^{1/2} \mathbf{P}_{Co}^{(L-1)/2} \mathbf{T}_{Co}^{1/2} \mathbf{S}^t| \\ Z_{Even} = \text{tr} |\mathbf{S} \mathbf{T}_{Co}^{1/2} \mathbf{P}_{Co}^{L/2-1} \mathbf{T}_{Co}^{1/2} \mathbf{T}_J \mathbf{T}_R \mathbf{S}^t| \\ Z_{Odd}^R = \text{tr} |\mathbf{S} \mathbf{T}_R^{1/2} \mathbf{P}_R^{(L-1)/2} \mathbf{T}_R^{1/2} \mathbf{S}^t|. \end{cases} \quad (5)$$

Following the calculations reported in the appendix analytical expressions for the free energy associated to these three contributions can be obtained. In analogy to results previously reported for more simple systems^{25,29} each of the free energies corresponding to the partition functions in Eq. (5) can be rewritten as a sum of three analytically separable parts

$$F_{Odd}^{Co} = F_b^{Co} + F_{end}^{Co} + F_{fs}^{Co} = -k_B T \left\{ \frac{L}{2} \ln(\lambda_{>}) + \ln \left[\frac{(M_{>}^{Co})^2}{\sqrt{\lambda_{>}}} \right] \right.$$

$$\left. + \ln \left[1 + \left(\frac{M_{\leq}^{Co}}{M_{>}^{Co}} \right)^2 \left(\frac{\lambda_{\leq}}{\lambda_{>}} \right)^{(L-1)/2} \right] \right\},$$

$$\begin{aligned}
F_{Even} &= F_b^{Even} + F_{end}^{Even} + F_{fs}^{Even} = -k_B T \left\{ \frac{L}{2} \ln(\lambda_>) \right. \\
&\quad \left. + \ln\left(\frac{2M_{>}^{Co} D_{>}}{\lambda_>}\right) + \ln\left[1 + \frac{M_{<}^{Co} D_{<}}{M_{>}^{Co} D_{>}} \left(\frac{\lambda_{<}}{\lambda_{>}}\right)^{L/2-1}\right] \right\}, \\
F_{Odd}^R &= F_b^R + F_{end}^R + F_{fs}^R = -k_B T \left\{ \frac{L}{2} \ln(\lambda_>) + \ln\left[\frac{(M_{>}^R)^2}{\sqrt{\lambda_>}}\right] \right. \\
&\quad \left. + \ln\left[1 + \left(\frac{M_{<}^R}{M_{>}^R}\right)^2 \left(\frac{\lambda_{<}}{\lambda_{>}}\right)^{(L-1)/2}\right] \right\}, \quad (6)
\end{aligned}$$

where $\lambda_>$ and $\lambda_{<}$ are the larger and the smaller eigenvalues of the product matrices in Eq. (4) and $(M_{>}^{Co})^2$, $(M_{<}^{Co})^2$, $(M_{>}^R)^2$, $(M_{<}^R)^2$, $D_{>}$, and $D_{<}$ are combinations of elements of the eigenvectors, as defined in the Appendix. The total free energy itself can now be separated into the same three contributions summing up the terms deriving from different chains

$$F_L = F_b + F_{end} + F_{fs} \quad (7)$$

with

$$\begin{aligned}
F_b &= F_b^{Co} + F_b^R + F_b^{Even}, \\
F_{end} &= F_{end}^{Co} + F_{end}^R + F_{end}^{Even}, \\
F_{fs} &= F_{fs}^{Co} + F_{fs}^R + F_{fs}^{Even}. \quad (8)
\end{aligned}$$

This separation has a physical meaning and can help in understanding the behavior of the system. The first of these three terms, F_b , which is proportional to the segment length L and thus the most important one for long chains, corresponds to the free energy of the infinite system in the zero dilution limit and is therefore considered a bulk contribution. The second, F_{end} , is independent of L and is a contribution given by the presence of surface (end point) spins at the end of the chains and obviously vanishes for zero dilution. The third term, F_{fs} , which decays exponentially with L and disappears in the infinite limit as the previous one, is the finite size contribution. It can be somewhat regarded as the contribution of small segments behaving as a whole, as appears from the following discussion.

In Fig. 1 we show the temperature dependence of the magnetic susceptibilities that arise from these three contributions and their role on the total susceptibility. Here it might be useful to point out that in the following we will always calculate and measure the susceptibility using its proper definition of $\chi = -\partial^2 F / \partial H^2$. This quantity is experimentally accessible via *ac* susceptibility measurements and its use is preferable, as it is not related to any linear regime assumption, to the often used “static” $\chi = M/H$ definition. Interestingly both χ_{end} and χ_{fs} can be negative: as the bulk progressively orders, before the peak in χ_b on lowering T , the residual thermal fluctuations become localized at the end point spins and thus the contribution χ_{end} is negative. A higher field would tend to align many spins in the bulk while some spins at the end points would align antiparallel to the field to maximize the entropic contribution due to the tem-

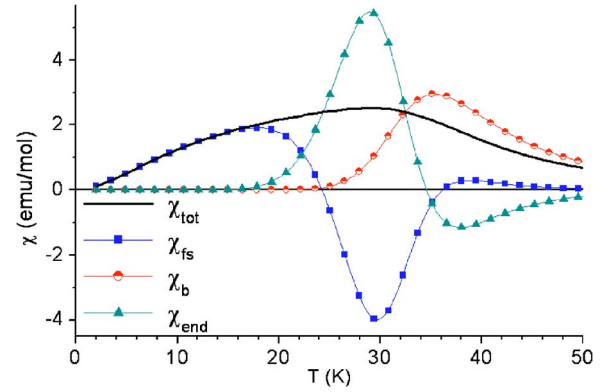


FIG. 1. (Color online) Different contributions to the magnetic susceptibility of an Ising ferrimagnetic chain in field calculated using the parameters $J/k_B = -90$ K, $H = 2$ kOe, $g_{Co} = 7$, $g_R = 2$, and $C = 1.2\%$. Blue squares represent the finite-size contribution, red circles the bulk contribution, green triangles the surface term, and the black line is the total susceptibility curve.

perature. Once the bulk contribution begins to decrease a small increase in the field aligns a great number of surface spins and entropy must accumulate into short segments of ordered spins not aligned with the field, thus giving a negative value of χ_{fs} . At even lower temperatures the main contribution to the susceptibility is then due to the aligning of these last short segments with the field. This fact can be easily shown by eliminating the contributions arising from the shorter segments, as shown in Fig. 2. The low temperature feature rapidly decreases as more and more short segments are eliminated from the calculation and it almost disappears when only chains with $L > 100$ are accounted for.

To this regard it is to be noted that, in contrast to the behavior of the dilute XY and classical Heisenberg models in field,³² for the Ising ferrimagnetic chain χ_{end} and χ_b decrease so rapidly, on lowering the temperature, that χ_{fs} can give rise to a second low temperature structure, which can become a well separated peak if a distribution in the concentration of defects is considered, as we will show in the next section. Thus, in this case, the contribution of finite size effects can be at least partially separated from the two other contributions, leading to a distinctive feature which can be experimentally investigated. This is a report of such a behavior in

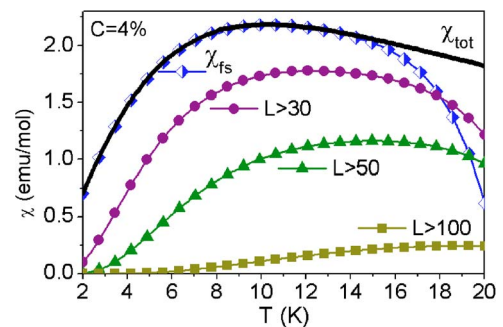


FIG. 2. (Color online) Variation of the low temperature structure of the magnetic susceptibility in field with the progressive elimination of longer segments of chain. All curves are calculated using the parameters $J/k_B = -90$ K, $H = 2$ kOe, $g_{Co} = 7$, $g_R = 2$, and $C = 4\%$.

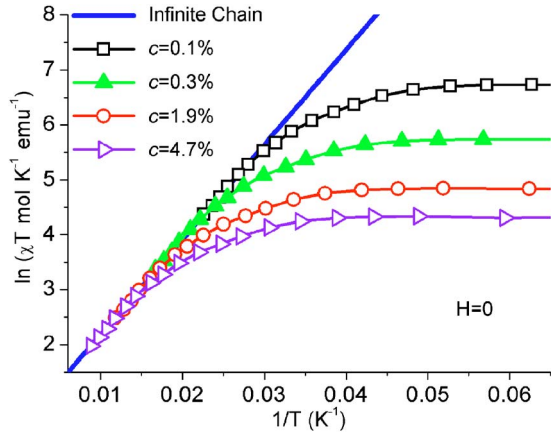


FIG. 3. (Color online) Theoretical scaling plots calculated at zero field for different concentrations of the dopant and using the parameters $J/k_B = -90$ K, $g_{Co} = 7$, and $g_R = 2$. The blue line represents calculated values for the infinite chain, black empty squares $C = 0.1\%$ missing sites, green full triangles $C = 0.3\%$, red open circles $C = 1.9\%$, and violet open triangles $C = 4.7\%$.

1D systems and a study to point out the rise of a structure, in the paramagnetic phase, directly related only to finite size effects. It must be stressed, anyhow, that the requirements needed to experimentally observe such a structure are indeed very difficult to fulfill. The behavior of the chains shall be dominated by a strong Ising anisotropy and the J'/J ratio must be sufficiently small to prevent interchain interactions from prevailing on intrachain ones at low temperature. Moreover, a big difference in the two g values is preferable in order to obtain significant effects. When both g values are set equal to 2 the low temperature feature becomes undistinguishable as the finite size contribution is found to be much broader and at lower temperature. The application of a field also plays an important role in separating the contributions, and the higher the g difference the lower the field needed to obtain a distinguishable low temperature feature. In the limiting case of an antiferromagnetic chain no such feature is observed and in no temperature range the finite size contribution can develop the low temperature shoulder to the main peak.

It can also be interesting to look at the behavior in zero field, although no low temperature shoulder can be clearly identified. It must actually be noticed that, in Ising systems, the rise of the susceptibility on lowering the temperature follows the growth of the correlation length with a rather distinctive exponential behavior, and $\chi T \propto e^{2J/k_B T}$.³³ A plot of $\ln(\chi T)$ vs $1/T$ will then give a straight line as long as the correlation length does not find a geometrical limit imposed by the defects. In Fig. 3 we plot the theoretical curves calculated for a ferrimagnetic Ising chain at different doping levels. The temperatures at which the deviation from the linear regime is observed are progressively higher for higher doping levels and this is due to the fact that, for samples with shorter distances between two defects, the correlation length will reach the geometrically imposed limit earlier. In this sense such a zero field scaling gives an idea of the behavior of the system and allows for easy schematic visualization of the effect of defects but, compared to the analysis of the

behavior in field it lacks the possibility to distinguish between the three different contributions, as some give negative susceptibility values. When making comparison to real systems, as the low temperature region can be strongly affected by defects, it also heavily relies on the assumption that the behavior of the system is still Ising in the high temperature region, while real systems tend to be in the Ising limit only at low temperatures. Such limitations do not affect, on the contrary, the previously discussed effects in field, which allow the observation of a distinctive low-temperature feature directly related to finite size effects that should be observable only for Ising spin systems, as discussed before.

Eventually it can be interesting to spend a few words on the effect of the alternation of different spin centers on Griffith's singularities. Griffith's argument²⁶ on the presence of singularities in the free energy of Ising dilute systems relies on the theorem of Yang and Lee²⁷ and states that in a dilute Ising model (of whatever dimensionality) the magnetization is a nonanalytic function of the magnetic field, at zero field, at a transition temperature T_G between the critical temperature of the pure system and that of the dilute one.

The role of defects in the occurrence of Griffith's singularities in ferromagnetic and antiferromagnetic chains was studied by Wortis,²⁵ who pointed out how the finite chain partition function vanishes for some imaginary values of the field, due to the finite size contribution to the free energy. In the 1D case both this kind of singularities and the trivial singularity at $T=0$, characteristic also of the infinite system, are present in the finite chain. This latter trivial singularity is connected to the branch cut belonging to $\Delta^{1/2}$ from Eq. (A5), which the F_b and F_{end} terms depend on, and is quite uninteresting, while the former arises from the remaining F_{fs} contributions. The finite size term of Eq. (8) is, in our case, deriving the sum of three different contributions from different chains. Following Eq. (A2) this leads to the presence of singularities whenever

$$\begin{cases} (\lambda_>)^{(L-1)/2} (M_>^{Co})^2 + (\lambda_<)^{(L-1)/2} (M_<^{Co})^2 = 0 \\ 2D_> M_>^{Co} (\lambda_>)^{L/2-1} + 2D_< M_<^{Co} (\lambda_<)^{L/2-1} = 0 \\ (\lambda_>)^{(L-1)/2} (M_>^R)^2 + (\lambda_<)^{(L-1)/2} (M_<^R)^2 = 0. \end{cases} \quad (9)$$

The roots of these equations all lie outside the physical domain but it is easy to see that now we have, instead of one essential singularity for any value of L , a splitting of the only root found in ferromagnets and antiferromagnets; this is due to the presence of the breaking of translational invariance, as in the cases already reported,²⁵ together with the doubling of the magnetic unit cell, which is an intrinsic characteristic of ferrimagnets. Physically this is due to the fact that segments of different composition (i.e., beginning with cobalt or with the radical) contribute in a slightly different way to the free energy of the system and the critical point is approached, for $T \rightarrow 0$, along different paths.

III. EXPERIMENTAL RESULTS ON CoPhOMe

It has long been predicted that 1D materials should easily display the influence of finite-size effects on their behavior, due to the presence of only one path along which the inter-

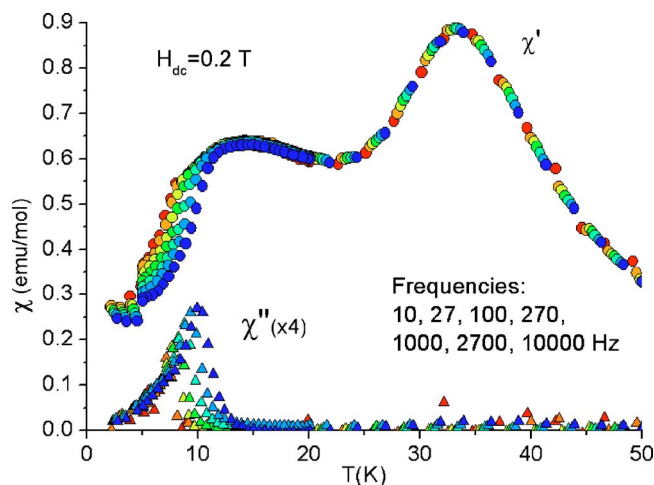


FIG. 4. (Color online) In-phase (χ' , shown as circles) and out-of-phase (χ'' , represented with triangles and magnified four times) components of the ac susceptibility for CoPhOMe. The measurement was performed on isooriented crystals in a static magnetic field $H_{dc}=0.2$ T along the c crystallographic axis and at different frequencies of the superimposed ac field, spanning a 10–10 000 Hz frequency range.

action can propagate, and a good number of theoretical works on the subject exist. Most of the direct experimental investigations attempted have been focused on a restricted range of materials, most noticeably Luttinger liquids,³⁴ TMMC,³⁵ and cupratelike systems.³⁶ Moreover most of them regard the use of neutron diffraction techniques to probe the presence of defects in the crystals and, rather surprisingly, it has never been possible to observe the emergence of a key feature in the thermodynamic properties to be associated only to finite-size effects. This is probably due to the choice of the materials and, in many cases, to the fact that either three or two dimensional ordering takes place before the correlation length becomes comparable to the length of the chains. Thus, to our knowledge, no experimental evidence has been reported of a behavior such as the one theoretically predicted in the previous section.

CoPhOMe [also called, more extensively, Co(hfac)₂NitPhOMe] chains are constituted by Co²⁺ ions (effective $s=1/2$ spins at low temperature) coordinated by two hexafluoroacetylacetonate (hfac) ligands and two nitronyl-nitroxide (NitPhOMe) radicals ($s=1/2$ spins) so as to form polymeric metallorganic chains with a wide inter-chain spacing, as described elsewhere.³⁷ Every single chain is structurally twisted in a helix that curls around the c axis and data seem to indicate the presence of noncollinearity of the Co²⁺ easy axes,³⁸ which form a chiral magnetic structure. The g factors of these two alternating $s=1/2$ magnetic centers have been shown to be very different,^{9,38} thus giving rise to ferrimagnetic behavior, while the J coupling has been described as an interaction with a strong Ising anisotropy, as often reported for Co²⁺ magnetic centers. This latter fact is at the basis of the strong Ising behavior of the system and, thus, of the slow dynamics found at low temperature.⁸

In Fig. 4 we report ac susceptibility measurements performed in a static field $H_{dc}=0.2$ T using a PPMS system

from Quantum Design. The out-of-phase ac susceptibility (χ'') shows a *single* peak at different temperatures, depending on the frequency used, below which the behavior is dominated by Glauber slow dynamics of the magnetization. The study of finite size effects in this dynamical region, which has led to a deeper understanding of the dynamics of the Ising model with finite chains and to the observation of multispin processes,²¹ deserves a theoretical frame and a treatment of its own and will thus be reported in a forthcoming study.³⁹ In the present work we will focus on the region above this temperature, at which the behavior of the system shows no frequency dependence and we will thus show only the measurements obtained for a single frequency, being implicit that data have also been acquired for several other frequencies. In this region the in-phase component (χ') clearly displays a peak at 33.5 K and a second one at about 14 K, just above the blocking temperature for all the frequencies used. As previously reported⁹ the system in this region is still in the paramagnetic phase and the only relevant interactions are those along the chains.

No 1D model which makes use of Born-von Kármán boundary conditions accounts for the presence of these two peaks which, on the contrary, can be explained by the classical treatment exposed in the previous part. To obtain clear evidence that this behavior is indeed due to the influence of finite size effects we decided to investigate the effect of the insertion of a controlled quantity of randomly placed diamagnetic impurities in the chains. We then chose, for chemical reasons, to substitute some of the cobalt magnetic centers with Zn²⁺ diamagnetic ions. We then prepared a number of doped samples by precipitation from solutions with different ratios of Zn(hfac)₂·2H₂O vs Co(hfac)₂·2H₂O. As already noted,⁴⁰ using this procedure the dopant can be inhomogeneously distributed among the crystals and even inside single crystals. These inhomogeneities can significantly affect the magnetic properties and we thus chose to measure the distribution of the dopant inside the crystals in order to directly observe possible concentration trends which, up to now, have been considered only on general and hypothetical basis.⁴⁰

The samples were then analyzed using an inductively coupled plasma-mass spectrometer (ICP-MS) coupled plasma and the PIXE technique with the external microbeam apparatus available at the accelerator of the INFN unit in Florence.⁴¹ The low minimum detection limits of the PIXE allowed us to find that no metals other than Co and Zn were present in concentration higher than 12 ppm and thus no appreciable contribution could rise from paramagnetic impurities. The Zn concentration was always found to be reproducible in crystals from the same batch (within a deviation of 5% on the mean concentration of dopant \bar{C}), but not reproducible in different syntheses. In the upper part of Fig. 5 we show, as an example, the results of the measurements performed on crystals obtained using an exactly identical synthetic procedure from two batches which contained the same starting Zn/Co ratio of 5%. At least ten different points were measured on every crystal and the doping can be considered homogeneous inside each batch, as each value lies within the standard deviation bars. On the contrary the doping is clearly not reproducible from one batch to another, being the differ-

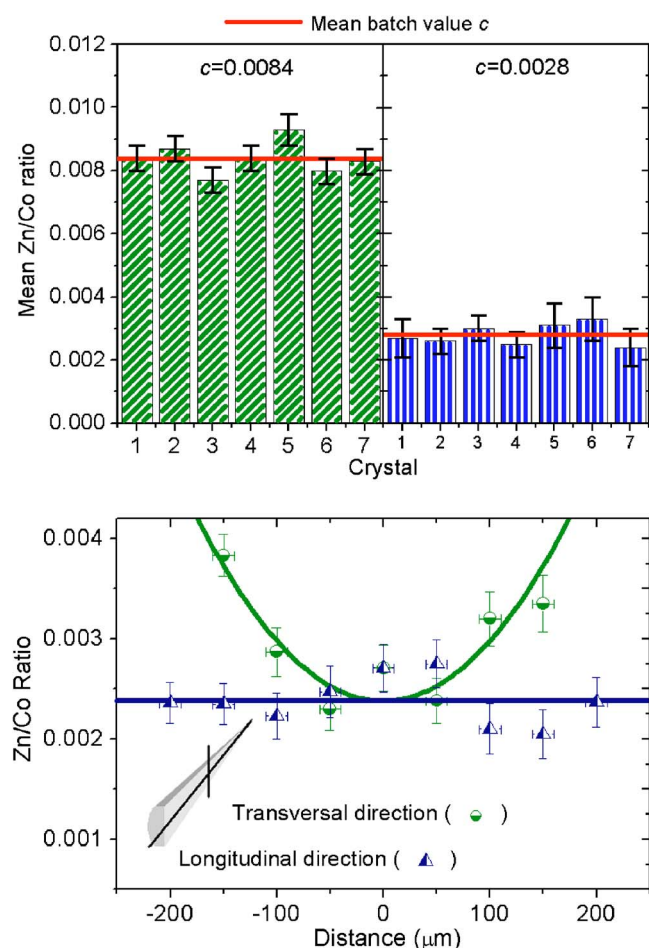


FIG. 5. (Color online) (top) Distribution of the dopant among the crystals obtained from two different batches containing the same 5% Zn/Co ratio in solution. The bars are the calculated standard deviations. (bottom) Zn/Co ratio in a single crystal of CoPhOMe. The distribution of the dopant is reported with blue triangles for the longitudinal direction, along the c axis, and with green circles along the transversal direction, perpendicular to the c axis. Lines are guides to the eye. In the drawing, in the bottom-left corner, one of the scanning geometries used is schematized.

ence of concentration between the two batches much larger than the deviation from the mean value in a single batch. Anyway it is interesting to note that, although the Zn content in the crystals was not reproducible in different batches, it was always found to be much lower (about ten times lower) than that of the starting solution. This indicates a lower tendency of the radical to bind Zn^{2+} ions than Co^{2+} ones, which is consistent with the fact that no Zn-nitronyl-nitroxide chain has been synthesized to date.

In the lower part of Fig. 5 we show one of the scans performed with the microbeam apparatus to analyze the concentration trend inside the crystals. The scans were performed longitudinally and transversally on sliced crystals, as shown in the figure. These scans revealed that the dopant is uniformly distributed along the c axis direction, while the concentration of Zn increases transversally going from the center to the edges. This observation is consistent with the acicular morphology of the crystals, which seem to grow

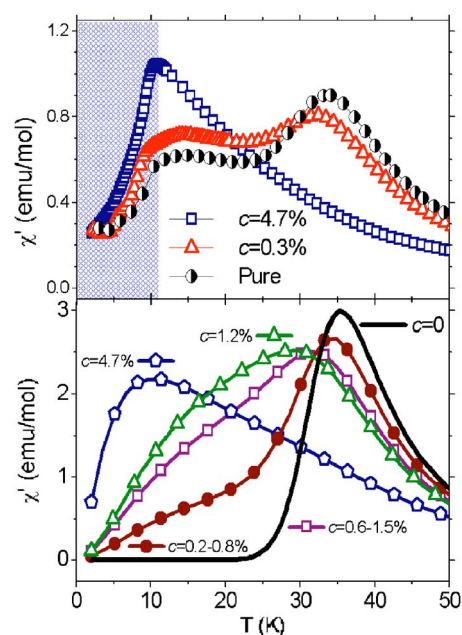


FIG. 6. (Color online) (top) Temperature dependence of the longitudinal magnetic ac susceptibility (2.7 kHz) measured at 2 kOe for the three different dopings indicated in the legend. In the shaded region we observe slow relaxation and $\chi'' > 0$. (bottom) Calculated susceptibility (parameters in the text) for different concentrations of impurities as indicated in the legend. A parabolic distribution is used, at low concentrations, to account for the observed transversal trend.

much more rapidly along the c axis, and the progressive enriching of the solutions in Zn content, due to the scarce reactivity of Zn with the radical. The same transversal trends were observed in crystals sliced along planes perpendicular to the c axis, thus excluding possible geometrical effects. The mean concentration of Zn inside the samples and observed Zn/Co ratios were also confirmed by ICP-MS coupled plasma measurements. The mean Zn/Co ratios of the magnetically investigated samples, \bar{c} , were 0.3%, 1.9%, and 4.7%, respectively, giving a range of average lengths \bar{L} between two Zn^{2+} ions variable from about 300 to almost 20 spins. Higher concentrations could not be obtained, presumably due to the aforementioned reactivity problems with Zn.

In the upper part of Fig. 6 we report the observed evolution with the concentration of the real component χ' of the ac magnetic susceptibility measured at 2.7 kHz in a static magnetic field of 0.2 kOe. The low temperature peak of the large anomalous structure present in the pure sample increases visibly with the reduction of \bar{L} and, at high doping, is the only one to survive. The high temperature peak, on the contrary, is more pronounced in the pure sample and decreases and shifts to lower temperatures as the concentration of Zn increases. In the shaded area dynamical effects dominate the behavior of the material.

These data can be at least qualitatively reproduced by the transfer matrix approach exposed in the previous section, as shown by the calculations reported in the lower part of Fig. 6, performed for $J/k_B = -90$ K, $H = 2$ kOe, $g_{\text{Co}} = 7$, and $g_R = 2$ and for different doping values. No distinction was made

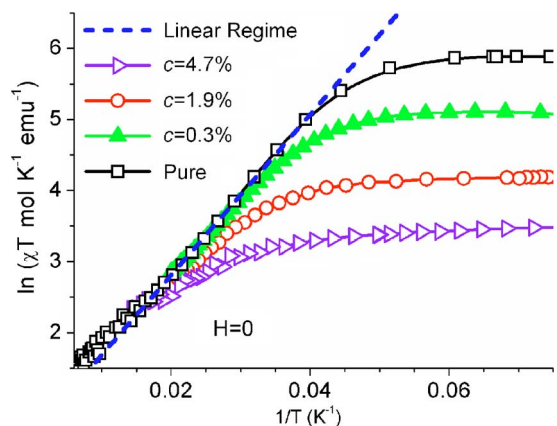


FIG. 7. (Color online) Scaling plot obtained for CoPhOMe. All data were taken in zero field and measured at a frequency of 27 Hz of the superimposed ac field on isooriented crystals along the c axis. Measurements were taken for different concentrations of the dopant: open squares represent the undoped sample, solid triangles $C = 0.3\%$, open circles $C = 1.9\%$, open triangles $C = 4.7\%$. The blue dashed line evidences the linear behavior observable between 55 and 26 K. The continuous lines are guides to the eye.

between breaks arising from defects on radical or from substituted cobalt sites, as the two contributions are almost the same even for very different g values. For the infinite chain we obtain only one peak, due to saturation effects, at $T \approx 34$ K and the dilution of the chain gives rise to the observed peak shift and to the development of the shoulder at about 15 K into a single peak at high doping.

Although complete quantitative agreement is not possible due to the helicoidal crystal structure of the CoPhOMe (Refs. 9 and 37) and the complexity of the Hamiltonian of the real system, the overall behavior and the anomalous double-peaked feature seem to be remarkably well reproduced by the schematic Hamiltonian of Eq. (1). This is especially true if one introduces, at concentrations in which both peaks are present, a parabolic distribution of the dopant, as observed in the analysis. At higher concentrations the behavior can be reproduced using either a distribution or a homogeneous doping, being the low temperature peak the only one to survive. Such an agreement seems to suggest a strongly dominant Ising behavior, which, despite the above-mentioned complications in the Hamiltonian, allows for at least the qualitative modeling of the main experimental features. It is then interesting to show how the complications inherent to the Hamiltonian of the experimental system do not really alter the Ising nature of the magnetic behavior performing the aforementioned scaling procedure plotting $\ln(\chi T)$ vs $1/T$. The results are plotted in Fig. 7 for both the undoped and the doped samples.

The expected linear behavior is observed in the undoped sample from 55 to 26 K, a much wider temperature range than that found in previously reported data³³ and this observation is then clear evidence that the system, at low temperatures, shows a very strong Ising-like anisotropy. The temperature of 55 K, above which we have deviation from this regime, is in agreement with the reported energy spacing of Co^{2+} ions. So the observed deviation has to be attributed to

the population of higher energy electronic levels of the metallic centers and, thus, to the fact that the spin 1/2 approximation with high anisotropy does not hold anymore.

The low temperature deviation from the linear regime, which is found at about 26 K for the pure sample, is consistent with a geometrical limitation of the correlation length due to the presence of defects. From the data, using $J/k_B = 90$ and 26 K as temperature of departure from the linear regime, an average length of the order of a thousand spins between two defects can be calculated, in overall agreement with the above estimation of the concentration of defects for the pure sample. The deviation from the linear regime is found, in the curves for the doped samples, at progressively higher temperatures for higher doping values. In these cases the three temperatures are also in agreement with the order of magnitude of the expected average segment length for the three observed dopings. Fitting of the linear regime for the pure system, also shown in the figure, gave a slope of 117 ± 2 K (with $R = 0.999$), thus leading to an estimation $J/k_B = -58$ K.

This value is in good agreement with previous analysis performed in the same temperature range with an infinite ferrimagnetic chain model,⁸ but is sensibly lower than the $J/k_B = -90$ value estimated from the above discussion of the low temperature region under field and also disagrees with the value extracted from the dynamics of the system, which was $J/k_B \approx -80$ K.²¹ Such data seem to indicate that although the system can be very well schematized with an Ising model below 55 K the behavior in the low temperature and high temperature regions is not exactly the same. This trend is expected to be quite common as a real magnetic system is never exactly described by the Ising model but approaches it only at low temperature. A spreading of the domain walls inside the chains is then expected at high temperatures, and this can lead to the observed discrepancy of J values. In many SCM compounds, as the Ising correlation length diverges exponentially, the low temperature region will probably be dominated by finite-size effects and thus the scaling plot will not allow for an estimation of the parameters of the Hamiltonian in the same temperature region at which the dynamics is observed. It is also to be noticed that the most appealing systems, i.e., those with a high barrier and thus high J values, will be those most affected by the geometrical breaking of the chains. For such systems it can become very difficult to individuate the linear regime, as this will be squeezed between a temperature region, where ions are not anisotropic, and the low-temperature regime, dominated by finite-size effects.

On the contrary the analysis of the behavior in field relies on features which appear at low temperature, right above the dynamical regime. Although we did not perform a real fitting procedure the estimated parameters which qualitatively reproduce the behavior are then in much better agreement to the values extracted from the dynamic properties. This analysis, which is applicable also to compounds with very high J values, can then give information that cannot be obtained by performing only the scaling plot.

Eventually it can be interesting to observe how the zero field data are connected to the measurements in an externally applied field and how the discussed low temperature struc-

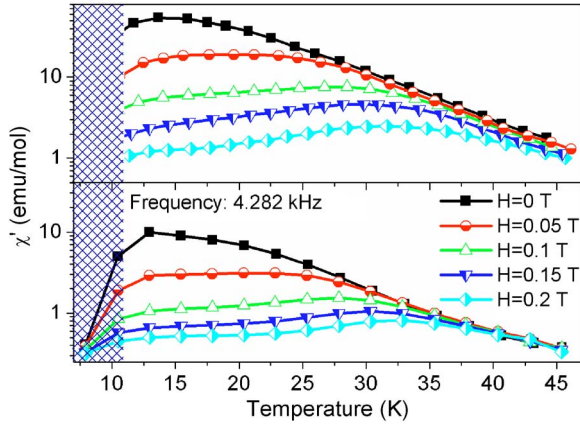


FIG. 8. (Color online) (top) Susceptibility calculated using the $C=0.6\text{--}1.5\%$ concentration range and the same parameters of Fig. 3. (bottom) Field evolution of χ' in CoPhOMe as measured on oriented crystals at 4.282 kHz frequency of the superimposed ac field. The same symbols and colors are used to indicate the field value of both calculated and experimental data: black squares, 0 T; red circles, 0.05 T; green up-triangles, 0.1 T; blue down-triangles, 0.15 T; cyan rhombuses, 0.15 T. The shaded area indicates, as in Fig. 6, the temperature region where dynamical effects are observable and $\chi'' > 0$.

tures grow with the field. To this aim we show, in Fig. 8, the field evolution of the χ' curve of CoPhOMe with the one calculated for a ferrimagnetic Ising chain with random dilution using the parameters reported in the caption. The data were obtained using a homemade ac probe.⁴² In both cases the only visible peak at zero field develops into the two previously discussed structures with increasing field. Noticeably the observed field evolution of the peaks is also reasonably well reproduced by the model.

IV. CONCLUSIONS

In this paper we have investigated the temperature and field dependence of the static susceptibility of a dilute ferrimagnetic chain in presence of a longitudinal external magnetic field. Supposing that the nonmagnetic impurities are randomly distributed and that they divide the chain into non-interacting segments, the free energy of the dilute system can be evaluated summing over all the contributions of the independent segments. We calculated these contributions with a transfer matrix approach and taking into account the distinction between segments beginning and/or ending with spins with different g values. Contrary to results previously obtained for ferromagnetic Heisenberg and XY chains,^{29,30,32} in the present case the finite size contribution, which decays exponentially with increasing length of the segment, results to be fundamental at low temperatures, giving rise to a second feature in the static susceptibility. In zero field the calculated scaling plots for $\ln(\chi T)$ vs $1/T$ predicts a discrepancy from the linear behavior at higher temperatures for higher concentrations of defects.

These theoretical predictions have been compared, with qualitative agreement, to *ac* magnetic measurements that we

have performed on samples of the SCM CoPhOMe, where some cobalt magnetic centers are randomly substituted with Zn^{2+} diamagnetic ions. With the aim of verifying the adequacy of the model to represent the real system we have used the PIXE with an external microbeam setup to analyze the profile of the concentration of the dopant inside single crystals. In all the investigated samples a uniform distribution of the nonmagnetic dopant along the chain was observed, while a concentration trend was observed transversally, in agreement with what has to be expected from the morphology of the crystals and the reactivity of the two metals. Such a distribution of the impurities was then inserted into the calculations, improving the agreement between the calculated and experimental curves.

Finally, we have shown that even if a clear Ising behavior is observed in the nominally pure system, this evidence can be totally obscured by the presence of nonmagnetic impurities.

ACKNOWLEDGMENTS

This work has benefited from stimulating discussions with A. Vindigni and P. A. Mandó. We also gratefully acknowledge financial support from German DFG, Italian MIUR, and CNR (FISR, FIRB, and PRIN grants), European EC RTN QuEMolNa-MRTN-CT-2003-504880, and Brazilian CNPq.

APPENDIX A

Analytical expressions for the three contributions to the free energy can be obtained with some calculations. First of all we must find the eigenvalues and eigenvectors of the product matrices defined by Eq. (4) and we shall define

$$\mathbf{A}_{\text{Co}}\mathbf{\Lambda}_{\text{Co}}\mathbf{A}_{\text{Co}}^{-1} = \mathbf{P}_{\text{Co}},$$

$$\mathbf{A}_{\text{Co}} = \begin{bmatrix} a_{>,+}^{\text{Co}} & a_{<,+}^{\text{Co}} \\ a_{>,-}^{\text{Co}} & a_{<,-}^{\text{Co}} \end{bmatrix}, \quad \mathbf{\Lambda}_{\text{Co}} = \begin{bmatrix} \lambda_{>}^{\text{Co}} & 0 \\ 0 & \lambda_{<}^{\text{Co}} \end{bmatrix},$$

$$\mathbf{A}_{\text{R}}\mathbf{\Lambda}_{\text{R}}\mathbf{A}_{\text{R}}^{-1} = \mathbf{P}_{\text{R}},$$

$$\mathbf{A}_{\text{R}} = \begin{bmatrix} a_{>,+}^{\text{R}} & a_{<,+}^{\text{R}} \\ a_{>,-}^{\text{R}} & a_{<,-}^{\text{R}} \end{bmatrix}, \quad \mathbf{\Lambda}_{\text{R}} = \begin{bmatrix} \lambda_{>}^{\text{R}} & 0 \\ 0 & \lambda_{<}^{\text{R}} \end{bmatrix}.$$

Note that the two eigenvalue matrices shall be identical, $\mathbf{\Lambda}_{\text{R}} = \mathbf{\Lambda}_{\text{Co}} = \mathbf{\Lambda}$, as the same solution for the infinite must be obtained whichever of the two products of Eq. (4) we choose as transfer matrix. Thus after some algebra we obtain

$$\begin{aligned} \lambda &= e^{2a_J} \cosh(a_{\text{Co}} + a_{\text{R}}) + e^{-2a_J} \cosh(a_{\text{Co}} - a_{\text{R}}) \\ &\pm [e^{4a_J} \cosh^2(a_{\text{Co}} + a_{\text{R}}) + e^{-4a_J} \cosh^2(a_{\text{Co}} - a_{\text{R}}) \\ &\quad + 2 \cosh^2(a_{\text{Co}}) + 2 \cosh^2(a_{\text{R}}) - 2 \cosh(4a_J)]^{1/2}. \end{aligned} \quad (\text{A1})$$

We can now rewrite the three expressions in Eq. (5) as

$$Z_L = \begin{cases} Z_{Odd}^{Co} = \text{tr} |\mathbf{S} \mathbf{T}_{Co}^{1/2} \mathbf{A}_{Co} \mathbf{\Lambda}^{(L-1)/2} \mathbf{A}_{Co}^{-1} \mathbf{T}_{Co}^{1/2} \mathbf{S}^t| = (\lambda_{>})^{(L-1)/2} (M_{>}^{Co})^2 + (\lambda_{<})^{(L-1)/2} (M_{<}^{Co})^2 \\ Z_{Even}^{Co} = \text{tr} |\mathbf{S} \mathbf{T}_{Co}^{1/2} \mathbf{A}_{Co} \mathbf{\Lambda}^{L/2-1} \mathbf{A}_{Co}^{-1} \mathbf{T}_{Co}^{1/2} \mathbf{T}_J \mathbf{T}_R \mathbf{S}^t| = 2M_{>}^{Co} (\lambda_{>})^{L/2-1} [a_{>,+}^{Co} e^{a_{Co}^2/2} \cosh(a_R + a_J) + a_{>,-}^{Co} e^{-a_{Co}^2/2} \cosh(a_R - a_J)] \\ \quad + 2M_{<}^{Co} (\lambda_{<})^{L/2-1} [a_{<,+}^{Co} e^{a_{Co}^2/2} \cosh(a_R + a_J) + a_{<,-}^{Co} e^{-a_{Co}^2/2} \cosh(a_R - a_J)] \\ Z_{Odd}^R = \text{tr} |\mathbf{S} \mathbf{T}_R^{1/2} \mathbf{A}_R \mathbf{\Lambda}^{(L-1)/2} \mathbf{A}_R^{-1} \mathbf{T}_R^{1/2} \mathbf{S}^t| = (\lambda_{>})^{(L-1)/2} (M_{>}^R)^2 + (\lambda_{<})^{(L-1)/2} (M_{<}^R)^2, \end{cases} \quad (\text{A2})$$

where we have used the following notation:

$$D_{>} = a_{>,+}^{Co} e^{a_{Co}^2/2} \cosh(a_R + a_J) + a_{>,-}^{Co} e^{-a_{Co}^2/2} \cosh(a_R - a_J),$$

$$D_{<} = a_{<,+}^{Co} e^{a_{Co}^2/2} \cosh(a_R + a_J) + a_{<,-}^{Co} e^{-a_{Co}^2/2} \cosh(a_R - a_J), \quad (\text{A3})$$

and

$$M_{>}^{Co} = a_{>,+}^{Co} e^{a_{Co}^2/2} + a_{>,-}^{Co} e^{-a_{Co}^2/2},$$

$$M_{<}^{Co} = a_{<,+}^{Co} e^{a_{Co}^2/2} + a_{<,-}^{Co} e^{-a_{Co}^2/2},$$

$$M_{>}^R = a_{>,+}^R e^{a_R^2/2} + a_{>,-}^R e^{-a_R^2/2},$$

$$M_{<}^R = a_{<,+}^R e^{a_R^2/2} + a_{<,-}^R e^{-a_R^2/2}. \quad (\text{A4})$$

We can now observe that, after a bit of manipulation on the above expressions, we need only calculate the values of $(a_{<,-})^2$, $(a_{>,-})^2$, $(a_{<,+})^2$, $(a_{>,+})^2$, $|a_{<,-} a_{<,+}|$ and $|a_{>,-} a_{>,+}|$ for both Co and R superscripts. To do that it is convenient to use a quantity Δ , which is analogous to the one introduced by Wortis²⁵ and invariant for Co and R suffixes

$$\Delta = 4[e^{4a_J} \cosh^2(a_{Co} + a_R) + e^{-4a_J} \cosh^2(a_{Co} - a_R) + 2 \cosh^2(a_{Co}) + 2 \cosh^2(a_R) - 2 \cosh(4a_J)] \quad (\text{A5})$$

which can also be used to easily express the eigenvalues

$$\lambda = e^{2a_J} \cosh(a_{Co} + a_R) + e^{-2a_J} \cosh(a_{Co} - a_R) \pm \frac{\Delta^{1/2}}{2}. \quad (\text{A6})$$

It leads to compact forms for the products and squares of elements

$$|a_{<,-}^{Co} a_{<,+}^{Co}| = |a_{>,-}^{Co} a_{>,+}^{Co}| = \frac{\cosh(a_{Co})}{\Delta^{1/2}},$$

$$|a_{<,-}^R a_{<,+}^R| = |a_{>,-}^R a_{>,+}^R| = \frac{\cosh(a_R)}{\Delta^{1/2}}, \quad (\text{A7})$$

$$(a_{<,-}^{Co})^2 = (a_{>,+}^{Co})^2 = \frac{1}{2} + \frac{e^{2a_J} \sinh(a_{Co} + a_R) - e^{-2a_J} \sinh(a_{Co} - a_R)}{\Delta^{1/2}},$$

$$(a_{>,-}^{Co})^2 = (a_{<,+}^{Co})^2 = \frac{1}{2} - \frac{e^{2a_J} \sinh(a_{Co} + a_R) - e^{-2a_J} \sinh(a_{Co} - a_R)}{\Delta^{1/2}},$$

$$(a_{<,-}^R)^2 = (a_{>,+}^R)^2 = \frac{1}{2} + \frac{e^{2a_J} \sinh(a_{Co} + a_R) + e^{-2a_J} \sinh(a_{Co} - a_R)}{\Delta^{1/2}},$$

$$(a_{>,-}^R)^2 = (a_{<,+}^R)^2 = \frac{1}{2} - \frac{e^{2a_J} \sinh(a_{Co} + a_R) + e^{-2a_J} \sinh(a_{Co} - a_R)}{\Delta^{1/2}}, \quad (\text{A8})$$

where before calculating the explicit expressions for these values, we have taken advantage of the fact that, being the product matrices of Eq. (4) symmetric, some of the above square values and products must be equal. Using these last expressions we can eventually rewrite the squares of Eq. (A4) in a more explicit form

$$(M_{>}^{Co})^2 = \cosh(a_{Co}) + \frac{e^{2a_J} \sinh(a_R + a_{Co}) \sinh(a_{Co}) + e^{-2a_J} \sinh(a_R - a_{Co}) \sinh(a_{Co}) + 4 \cosh(a_{Co})}{2\Delta^{1/2}},$$

$$(M_{<}^{Co})^2 = \cosh(a_{Co}) - \frac{e^{2a_J} \sinh(a_R + a_{Co}) \sinh(a_{Co}) + e^{-2a_J} \sinh(a_R - a_{Co}) \sinh(a_{Co}) + 4 \cosh(a_{Co})}{2\Delta^{1/2}},$$

$$(M_{>}^R)^2 = \cosh(a_R) + \frac{e^{2a_J} \sinh(a_{Co} + a_R) \sinh(a_R) + e^{-2a_J} \sinh(a_{Co} - a_R) \sinh(a_R) + 4 \cosh(a_R)}{2\Delta^{1/2}},$$

$$(M_{<}^R)^2 = \cosh(a_R) - \frac{e^{2a_J} \sinh(a_{Co} + a_R) \sinh(a_R) + e^{-2a_J} \sinh(a_{Co} - a_R) \sinh(a_R) + 4 \cosh(a_R)}{2\Delta^{\frac{1}{2}}}. \quad (\text{A9})$$

-
- *Author to whom correspondence should be addressed. Email address: lapo.bogani@unifi.it
- †Author to whom correspondence should be addressed. Email address: roberta.sessoli@unifi.it
- ‡Present address: Institut de Chimie de la Matière Condensée de Bordeaux, CNRS UPR 9048, avenue du Docteur Schweitzer 87, 33608 Pessac Cedex, France.
- ¹F. D. M. Haldane, Phys. Rev. Lett. **50**, 1153 (1983); **93**, 206602 (1983).
- ²H. Shiba, T. Sakai, B. Lthi, W. Palme, and M. Sieling, J. Magn. Magn. Mater. **140-144**, 1590 (1995), and references therein.
- ³H. J. Mikeska and M. Steiner, Adv. Phys. **40**, 191 (1991).
- ⁴*Magnetism: Molecules to Materials IV*, edited by J. S. Miller and M. Drillon (Wiley, Chichester, 2003).
- ⁵ *π -Electron Magnetism: From Molecules to Magnetic Materials*, Structure and Bonding Series Vol. 100, edited by J. Veciana (Springer-Verlag, New York, 2001), and references therein.
- ⁶M. Affronte, A. Caneschi, C. Cucci, D. Gatteschi, J. C. Lasjaunias, C. Paulsen, M. G. Pini, A. Rettori, and R. Sessoli, Phys. Rev. B **59**, 6282 (1999).
- ⁷R. J. Glauber, J. Math. Phys. **4**, 294 (1963).
- ⁸A. Caneschi, D. Gatteschi, N. Lalioti, C. Sangregorio, R. Sessoli, G. Venturi, A. Vindigni, A. Rettori, M. G. Pini, and M. Novak, Angew. Chem., Int. Ed. **40**, 1760 (2001); Angew. Chem. **113**, 1810 (2001).
- ⁹A. Caneschi, D. Gatteschi, N. Lalioti, C. Sangregorio, R. Sessoli, G. Venturi, A. Vindigni, A. Rettori, M. G. Pini, and M. A. Novak, Europhys. Lett. **58**, 771 (2002).
- ¹⁰D. Gatteschi and R. Sessoli, Angew. Chem., Int. Ed. **42**, 268 (2003); Angew. Chem. **115**, 278 (2003).
- ¹¹R. Clèrac, H. Miyasaka, M. Yamashita, and C. Coulon, J. Am. Chem. Soc. **124**, 12837 (2002).
- ¹²R. Lescouëzec, J. Vaissermann, C. Ruiz-Perez, F. Lloret, R. Carrasco, M. Julve, M. Verdaguer, Y. Dromzee, D. Gatteschi, and W. Wernsdorfer, Angew. Chem., Int. Ed. **42**, 1483 (2003); Angew. Chem. **115**, 1521 (2003).
- ¹³T. Liu, D. Fu, S. Gao, Y. Zhang, H. Sun, G. Su, and Y. Liu, J. Am. Chem. Soc. **125**, 13976 (2003).
- ¹⁴L. M. Toma, R. Lescouëzec, F. Lloret, M. Julve, J. Vaissermann, and M. Verdaguer, Chem. Commun. (Cambridge) **2003**, 1850 (2003).
- ¹⁵E. Pardo, R. Ruiz-Garcia, F. Lloret, J. Faus, M. Julve, Y. Journaux, F. Delgado, and C. Ruiz-Perez, Adv. Mater. (Weinheim, Ger.) **16**, 1597 (2004).
- ¹⁶J. P. Costes, J. M. Clemente-Juan, F. Dahan, and J. Milon, Inorg. Chem. **43**, 8200 (2004).
- ¹⁷Z. M. Sun, A. V. Prosvirin, H. H. Zhao, J. G. Mao, and K. R. Dunbar, J. Appl. Phys. **97**, 10B305 (2005).
- ¹⁸D. Hone, P. A. Montano, T. Tonegawa, and Y. Imry, Phys. Rev. B **12**, 5141 (1975).
- ¹⁹S. Eggert, I. Affleck, and M. D. P. Horton, Phys. Rev. Lett. **89**, 047202 (2002).
- ²⁰M. Hagiwara, K. Katsumata, I. Affleck, B. I. Halperin, and J. P. Renard, Phys. Rev. Lett. **65**, 3181 (1990).
- ²¹L. Bogani, A. Caneschi, M. Fedi, D. Gatteschi, M. Massi, M. A. Novak, M. G. Pini, A. Rettori, R. Sessoli, and A. Vindigni, Phys. Rev. Lett. **92**, 207204 (2004).
- ²²M. Macciò, A. Rettori, and M. G. Pini, Phys. Rev. B **31**, 4187 (1985).
- ²³M. Macciò, A. Rettori, and M. G. Pini, Phys. Rev. Lett. **55**, 1630 (1985).
- ²⁴P. A. Mandó, in *Encyclopedia of Analytical Chemistry*, edited by R. A. Meyers (Wiley, Chichester, 2000), pp. 12708–12740.
- ²⁵M. Wortis, Phys. Rev. B **10**, 4665 (1974).
- ²⁶R. B. Griffiths, Phys. Rev. Lett. **23**, 17 (1969).
- ²⁷C. N. Yang and T. D. Lee, Phys. Rev. **87**, 404 (1952); **87**, 410 (1952).
- ²⁸F. Matsubara, K. Yoshimura, and S. Katsura, Can. J. Phys. **51**, 1053 (1973).
- ²⁹M. G. Pini and A. Rettori, Phys. Lett. A **127**, 70 (1988).
- ³⁰G. Q. Hu and A. R. McGurn, Phys. Rev. B **34**, 7836 (1986).
- ³¹J. P. Boucher, F. Mezei, L. P. Regnault, and J. P. Renard, Phys. Rev. Lett. **55**, 1778 (1985).
- ³²M. G. Pini and A. Rettori, in *Fundamental and Applicative Aspects of Disordered Magnetism*, edited by P. Allia, D. Fiorani, and L. Lanotte (World Scientific, Singapore, 1989), pp. 1–29.
- ³³C. Coulon, R. Clèrac, L. Lecren, W. Wernsdorfer, and H. Miyasaka, Phys. Rev. B **69**, 132408 (2004).
- ³⁴M. Bockrath, D. H. Cobden, J. Lu, A. G. Rinzler, R. E. Smalley, L. Balents, and P. L. McEuen, Nature (London) **397**, 598 (1999).
- ³⁵H. Asakawa, M. Matsuda, K. Minami, H. Yamazaki, and K. Katsumata, Phys. Rev. B **57**, 8285 (1998).
- ³⁶G. Xu, G. Aeppli, M. E. Bisher, C. Broholm, J. F. DiTusa, C. D. Frost, T. Ito, K. Oka, R. L. Paul, H. Takagi, and M. M. J. Treacy, Science **289**, 419 (2000).
- ³⁷A. Caneschi, D. Gatteschi, N. Lalioti, C. Sangregorio, and R. Sessoli, J. Chem. Soc. Dalton Trans. **21**, 3907 (2000).
- ³⁸A. Caneschi, D. Gatteschi, N. Lalioti, R. Sessoli, L. Sorace, V. Tangoulis, and A. Vindigni, Chem.-Eur. J. **8**, 286 (2002).
- ³⁹A. Vindigni *et al.* (unpublished).
- ⁴⁰C. Dupas and J. P. Renard, Phys. Rev. B **18**, 401 (1978).
- ⁴¹M. Massi *et al.*, Nucl. Instrum. Methods Phys. Res. B **190**, 276 (2002).
- ⁴²S. Midollini, A. Orlandini, P. Rosa, and L. Sorace, Inorg. Chem. **44**, 2060 (2005).